ELSEVIER

Thermochimica Acta 282/283 (1996) 443–452

thermochimica acta

Kinetic analysis of the isothermal crystallization of an *n*-alkane and polyethylene observed by simultaneous DSC/FT-IR/WAXD measurement[1]

Hirohisa Yoshida [a,*], Yutaka Ichimura [b], Ryoichi Kinoshita [b], Yoshihiko Teramoto [b]

[a] *Department of Industrial Chemistry, Tokyo Metropolitan University, Minami-Ousawa, Hachiouji, Tokyo 192-03, Japan*

[b] *Seiko Instruments, Inc., Scientific Instruments Division, Nakase 1–8, Mihama-ku, Chiba 261, Japan*

Abstract

The isothermal crystallization process of *n*-hexatriacontane ($C_{36}H_{74}$) and high-density polyethylene (HDPE) was observed by simultaneous DSC/FT-IR and DSC/WAXD measurements. For $C_{36}H_{74}$, the formation of the trans-conformation and the crystallization exothermic peak of the hexagonal phase from the melt were observed at the same time. The absorption band due to the rocking mode vibration of the methylene group was split at the transformation from the hexagonal phase to the modified monoclinic phase. In the case of HDPE, the formation of the trans-conformation started before the observation of the crystallization exothermic peak. When the crystallization exothermic peak was observed, about 60% of trans-conformation was already formed. The conformational transition from the gauche-form to the trans-form was recognized as a phenomenon occurring before the crystal growth of HDPE.

Keywords: Crystallization; DSC/FT-IR simultaneous measurement; Kinetics; Nucleation; Polyethylene

1. Introduction

The dynamics of ordering formation under non-equilibrium have been studied in this recent decade. The crystallization of a polymer, one of these phenomena, shows

* Corresponding author. Tel: + 81-426-77-2844; fax: + 81-426-77-2821; e-mail: yoshida-hirohisa@c.metro-u.ac.jp

[1] Dedicated to Takeo Ozawa on the Occasion of his 65th Birthday.

SSDI 0040-6031(96)02830-4

a drastic structural change; a randomly entangled one-dimensional molecule forms an ordered lattice with a critical side (nucleation), a crystal nucleus grows and forms lamellar crystals (crystal growth), and then the crystal lamellae form a spherulite with a size 10^4 times as large as the lamellar crystals (spherulite growth) [1]. Many researchers have reported the kinetic analysis of the crystal growth of polymers using differential scanning calorimetory (DSC) under both isothermal and scanning conditions [2–7]. However, DSC gives little information on the nucleation process because heat flow is barely observed during the nucleation of polymers. Therefore, there have been few experimental analyses reported for the nucleation of polymers.

Recently, Imai et al. [8,9] reported that a large-scale density fluctuation occurred in the induction period of crystallization of poly(ethylene terephthalate) from the glassy state. This large-scale density fluctuation observed in the induction period of crystallization is also reported for metal and colloid crystals [10]. Using a lattice model, Flory predicted theoretically the presence of a molecular ordering process before the start of crystal growth in polymers [11]. In other words, randomly entangled molecules align parallel to each other during the induction period or the nucleation process of crystallization of a polymer. It is expected that a conformational transition occurs before the crystal growth process of polymers.

The combined use of thermal analysis and X-ray scattering measurements is employed to analyze complex phase transition behaviors. Several groups have applied the simultaneous measurement of thermal analysis and X-ray scattering at synchrotron facilities [12–16]. We have improved the simultaneous differential scanning calorimetry (DSC) and small angle X-ray analysis (SAXS) measurement [17,18]; the sensitivity and accuracy of the DSC of the improved simultaneous DSC/SAXS instrument is comparable with conventional DSC. The detail of this simultaneous DSC/SAXS measurement instrument have been reported [18]. Using this DSC/SAXS instrument, we have analyzed the phase transition behavior of organic materials with polymorphism [19]. Furthermore, the simultaneous measurement was expanded to wide-angle X-ray scattering (WAXD) and Fourier transform infrared spectroscopy (FT-IR) in this study in order to analyze the isothermal crystallization process of an *n*-alkane and polyethylene.

2. Experimental

Hexatriacontane ($C_{36}H_{74}$), 99.8% purity, supplied by Tokyo Kasei Co. Ltd., and high-density polyethylene (HDPE) supplied by Polysciences, Inc., USA, were used throughout the experiment. Isothermal crystallization was carried out at pre-determined temperatures by cooling at 40 K min^{-1} from 353 K for $C_{36}H_{74}$ and from 418 K for HDPE after holding in the molten state for 2 min. Samples ranging between 1 and 3 mg were clamped in aluminum sample vessels manufactured for the simultaneous DSC/SAXS instrument [18]. Samples, which were held between two sheets of 10-μm-thick aluminum film for the DSC/WAXD measurment and between two KBr disks with 0.5 mm thickness for the DSC/FT-IR measurement, were put in aluminum vessels and clamped with lids.

The simultaneous DSC/X-ray scattering measurement instrument [18] was used for the simultaneous DSC/FT-IR and the simultaneous DSC/WAXD measurements. The simultaneous DSC/FT-IR and DSC/WAXD measurements were carried out by setting the DSC/SAXS instrument on the goniometer of the WAXD optics of the Mac Science model SRA MXP-18 X-ray instrument and on the JAS.CO FT-IR model 700. An FT-IR spectrum was obtained in the wavenumber range from 4,000 to 400 cm^{-1} with 4 cm^{-1} of resolution. A WAXD profile was obtained in transmission mode using a scintillation counter and a radial diffractometer scanned in the scattering angle (2θ) range from 19° to 24° at 15° min^{-1}. One FT-IR spectrum and WAXD profile required about 15 s and 24 s to measure and save in the work station under this scanning condition, respectively.

3. Results and discussion

3.1 n-*Hexatriacontane*

The solution-grown crystal of $C_{36}H_{74}$ was in the monoclinic form (M-phase) at room temperature, and the M-phase transformed to the modified monoclinic phase by tilting of the end methyl group (C-phase). With increasing temperature, the C-phase transformed to the hexagonal phase (H-phase) [20–22]. The transition temperatures evaluated as a crossing of the base line and transition slope by DSC at 1 K min^{-1} were 344.3 K (M to C), 345.2 K (C to H) and 346.7 K (H to liquid) on heating. The transition temperatures, determined as a crossing of the base line and transition slope on cooling at 1 K min^{-1} were 346.7 K (liquid to H), 344.7 K (H to C) and 344.2 K (C to M). On isothermal crystallization, two exothermic transition peaks were observed at temperatures between 345.1 and 344.7 K, and one exothermic peak was observed in the temperature region from 346.5 to 345.6 K.

The DSC exothermic peak and FT-IR spectrum change of $C_{36}H_{74}$ during isothermal crystallization at 345.9 K observed by simultaneous DSC/FT-IR measurement are shown in Fig. 1. DSC required 35 s to estabilish a stable base line, and then two sharp exothermic peaks were observed at around 50 s and 80 s. The first exothermic peak at around 50 s was due to the crystallization of H-phase from the molten state, and the second at around 80 s was the result of transformation of the C-phase from the H-phase. After the second exothermic peak, the third broad exothermic peak continued from 100 s to 150 s, and then the stable base line was observed.

The absorption band at around 720 cm^{-1} was assigned to the rocking mode vibration of the methylene group in the trans-conformation [23]. With continued crystallization, the absorbance of the band at 720 cm^{-1} increased and an absorption band at 730 cm^{-1} appeared when the transition from H-phase to C-phase occurred. The absorption band at 730 cm^{-1} appeared as the result of splitting the rocking mode vibration to B_{1u} and B_{2u} modes, which are parallel to the *a*- and *b*-axes of the crystal, respectively, caused by intermolecular interactions in crystallites [23]. In other words, the increase in the absorption band observed at 720 cm^{-1} indicated an increase in the

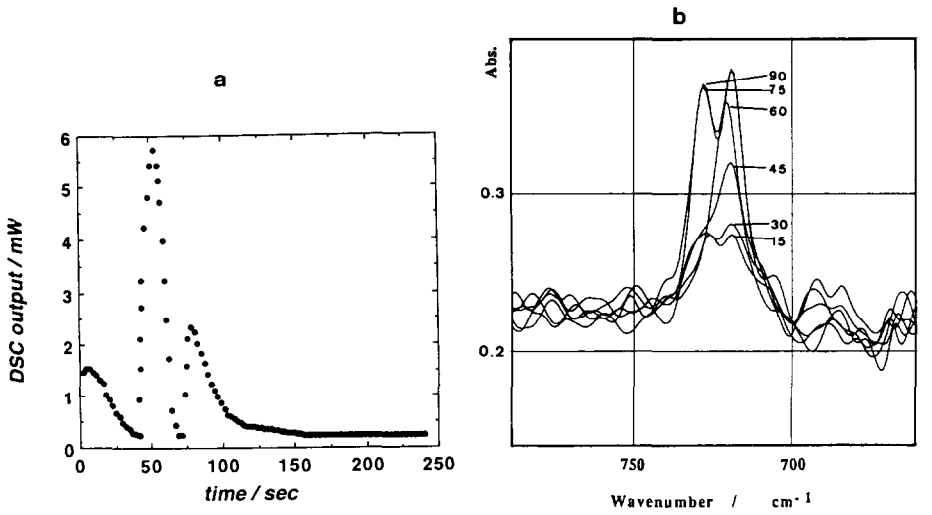

Fig. 1. Simultaneous DSC (a) and FT-IR (b) results of $C_{36}H_{74}$ during isothermal crystallization at 344.9 K. The numbers in (b) show the crystallization times.

trans-conformation and the appearance of the split band at 730 cm^{-1} suggested crystal perfection.

From the DSC exothermic peak, the fraction of the crystallized part $(1-\theta)_C$ was evaluated by the equation

$$(1-\theta)_C = \Delta H(t)/\Delta H(\infty) \tag{1}$$

Here, θ, $\Delta H(t)$ and $\Delta H(\infty)$ indicate the fraction uncrystallized, the portion of exothermic heat at time t, and the total exothermic heat during isothermal crystallization, respectively. In a similar manner, the fraction of trans-conformation, $(1-\theta)_{720}$, was evaluated from the IR spectra using the equation

$$(1-\theta)_{720} = \Delta A_{720}(t)/\Delta A_{720}(\infty) \tag{2}$$

$$\Delta A_{720}(t) = A_{720}(t) - A_{720}(0)$$

$$\Delta A_{720}(\infty) = A_{720}(\infty) - A_{720}(0)$$

where θ, $A_{720}(0)$, $A_{720}(t)$ and $A_{720}(\infty)$ denote the fraction unchanged, and the absorbance at 720 cm^{-1} at time 0, t and infinity, respectively. Similarly, the change in the trans-conformation was evaluated using the absorption band at 730 cm^{-1}.

The isothermal crystallization process of $C_{36}H_{74}$ at 344.9 K observed by simultaneous DSC/FT-IR measurement is shown in Fig. 2. The transition process of the first exothermic peak due to crystallization of H-phase from the molten state shows a typical sigmoidal shape. The transition process of the second exothermic peak seems to be composed of two processes occurring around 100 s. The ratio of the total transition heat of the first exothermic peak against the second exothermic peak, including the broad exothermic peak, was about 2.3 for three different isothermal

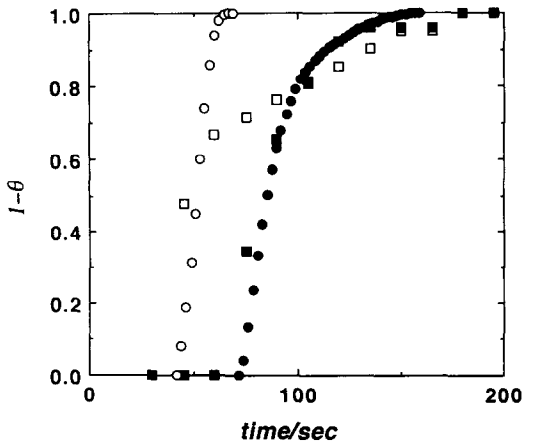

Fig. 2. Changes in crystallinity: ○, $(1-\theta)_C$ of the transition from the melt to the hexagonal phase; ●, $(1-\theta)_C$ of the transition from the hexagonal to the monoclinic phase; and the fraction of trans – conformation: □, $(1-\theta)_{720}$; and ■, $(1-\theta)_{730}$ of $C_{36}H_{74}$ during isothermal crystallization at 344.9 K.

crystallization measurements. This value showed a good agreement with the DSC results measured on heating, in which the ratio of the transition heat of the melting of the H-phase against the total transition heat of transformation of the C-phase and the M-phase was 2.3. [8]. From these results, the broad exothermic peak observed after the second exothermic peak is due to the transition from C-phase to M-phase.

The increase in absorbance at 720 cm^{-1} began when the first exothermic peak started. The second exothermic peak and the increase in the absorption peak at 730 cm^{-1} started at the same time. The second and third exothermic processes were also separated by a change in $(1-\theta)$ evaluated from the absorption band at 730 cm^{-1}. The increase in the absorbance at 720 cm^{-1} was mainly observed during the crystallization of the H-phase from the molten state, and then continued during the transformation of the C-phase and the M-phase. In other words, only 60% of trans-conformation in $C_{36}H_{74}$ was established during the crystallization of the H-phase from the melt. This suggests that the H-phase included much conformational disorder. In fact, the WAXD profile of the H-phase was broader than that of the C-phase [18]. However, the absorption band at 730 cm^{-1} increased mainly at the transformation of the C-phase to the H-phase. Furthermore, the increase of the absorption band at 730 cm^{-1} was barely observed for isothermal crystallization at temperatures above 345.6 K in which only the first exothermic peak due to crystallization of the H-phase was observed. The amount of trans-conformation and the symmetrical order of the molecular packing in the crystal increased with the transformation from H-phase to C-phase. The split of the absorption peak assigned to the trans-conformation was observed at the transition from the H-phase to the C-phase as a result of an improvement in molecular packing.

The half time ($t_{1/2}$) of transition was evaluated from the normalized transition plot shown in Fig. 2. The evaluated $t_{1/2}$ from the DSC exothermic peak ($t_{1/2H}$) and $t_{1/2}$ from the FT-IR spectrum ($t_{1/2T}$) for isothermal crystallization at various temperatures are

plotted in Fig. 3. The value of $t_{1/2H}$ evaluated from the heat of transition from the melt to the H-phase was almost the same as $t_{1/2T}$ evaluated from the absorption band at 720 cm^{-1}. Furthermore, the value of $t_{1/2H}$ evaluated from the heat of transition from the H-phase to the C-phase was almost the same as that of $t_{1/2T}$ evaluated from the absorption band at 730 cm^{-1}. These facts suggest that the conformational transition from the gauche-form to the trans-form started at the same time as the crystal growth of H-phase, and that the stable molecular packing was induced by the transition from the H-phase to the C-phase for $C_{36}H_{74}$.

3.2. Polyethylene

Changes in the FT-IR spectrum and WAXD profile of HDPE during isothermal crystallization at 395 K observed by simultaneous DSC/FT-IR and DSC/WAXD measurements are shown in Fig. 4. The DSC melting peak temperature of this sample was 408.2 K. Isothermal DSC curves observed by both measurements showed good agreement within experimental error. With continued crystallization, the absorption band at 720 cm^{-1} shifted slightly to the high wavenumber side and the absorbance of this band increased. The transition exothermic peak was completed at 600 s after holding at 395 K; however, no splitting of the absorption band at 720 cm^{-1} was observed. When the sample crystallized at 395 K was cooled to room temperature, the doublet of absorption bands at 720 and 730 cm^{-1} was observed. The WAXD profile at time 0 to 100 s showed a typical amorphous halo pattern. The diffraction peak of the (110) plane, scattering angle $2\theta = 20.9°$, and the diffraction peak of the (200) plane, $2\theta = 22.7°$, appeared at 200 s, and the diffraction intensity of both diffraction peaks increased with crystallization.

The fractions of the crystallized part, $(1-\theta)_C$ and the trans-conformation, $(1-\theta)_{720}$, were obtained. As with Eqs. (1) and (2), $(1-\theta)_C$ was also evaluated from WAXD

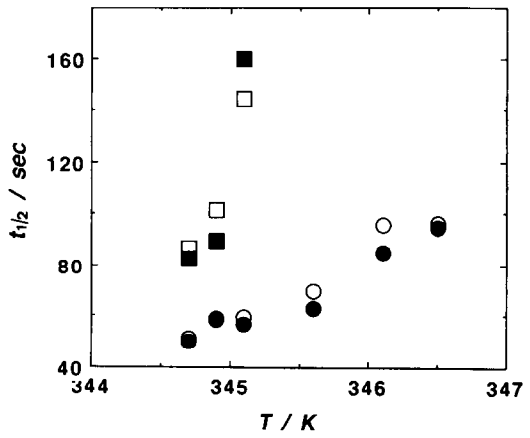

Fig. 3. Temperature dependence of the half time ($t_{1/2}$) evaluated from the first (○) and second (●) exothermic peaks, and from the absorbance at 720 cm^{-1} (□) and 730 cm^{-1} (■) for $C_{36}H_{74}$.

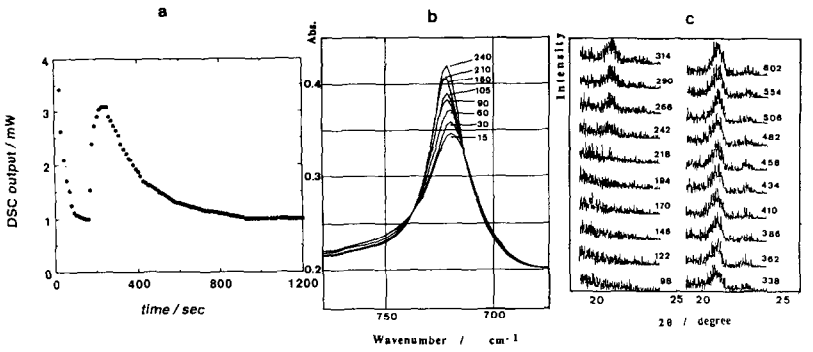

Fig. 4. Simultaneous DSC/FT-IR and DSC/WAXD results of HDPE during isothermal crystallization at 395 K: a, DSC; b, FT-IR; c, WAXD. The numbers in the figure show the crystallization times.

profiles, $(1-\theta)_{CX}$, by the equation

$$(1-\theta)_{CX} = \Delta I_{110}(t)/\Delta I_{110}(\infty) \tag{3}$$

$$\Delta I_{110}(t) = I_{110}(t) - I_{110}(0)$$

$$\Delta I_{110}(\infty) = I_{110}(\infty) - I_{110}(0)$$

where θ, $I_{110}(0)$, $I_{110}(t)$ and $I_{110}(\infty)$ denote the fraction unchanged, and the X-ray diffraction intensity of the (110) plane at times 0, t and infinity, respectively. The Avrami constants (n) obtained by the Avrami-Evofeev equation, $\theta = \exp(-Zt^n)$ for the crystallization exothermic peak of HDPE were in the range 3.8–4.0. These values suggest that crystal growth of HDPE occurred three dimensionally with homogeneous nucleation.

The isothermal crystallization process of HDPE at 395 K observed by the simultaneous DSC/FT-IR and DSC/WAXD measurements is shown in Fig. 5. The crystallization exothermic peak and the increase of the absorption band at 720 cm^{-1} started at the same time for $C_{36}H_{74}$; however, the increase of the absorption band at 720 cm^{-1} started earlier than the crystallization exothermic peak for HDPE. The absorption band at 720 cm^{-1} started to increase at 30 s, and then the crystallization exothermic peak started at 100 s when 60% of trans-conformation was reached. Furthermore, the diffraction peak of the (110) plane was observed at 200 s, when the crystallization exothermic heat approached 50% of the total crystallization heat. Although details of the crystallization behavior at other crystallization temperatures differed slightly from that at 395 K, the order of appearance—absorption band at 720 cm^{-1}, exothermic peak, and then the diffraction peak of (110) plane—was commonly observed for HDPE.

The half-time of each process was determined by the method described above. The temperature dependence of the half-time ($t_{1/2}$) evaluated from the crystallization exothermic peak ($t_{1/2H}$), the absorbance at 720 cm^{-1} ($t_{1/2T}$) and the half-time from the WAXD peak of the (110) plane ($t_{1/2X}$) for HDPE are shown in Fig. 6. For all crystallization temperatures examined in this study, the formation of trans-conformation preceded the crystal growth process for HDPE. With increasing crystallization

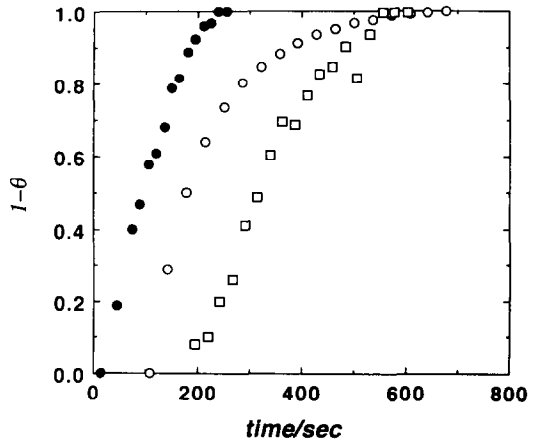

Fig. 5. Changes in crystallinity observed by DSC exothermic and WAXD peak, $(1-\theta)_C$ (○) and $(1-\theta)_{CX}$ (□), and fraction of trans-conformation, $(1-\theta)_{720}$ (●), of HDPE during isothermal crystallization at 395 K.

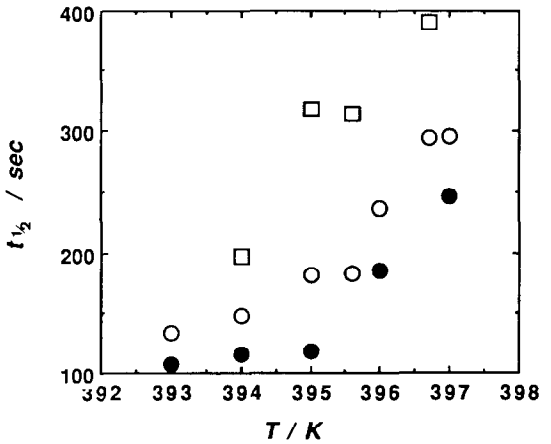

Fig. 6. Temperature dependence of the half-time ($t_{1/2}$) evaluated from the crystallization exothermic peak (○), the absorbance at 720 cm^{-1} (●) and from the WAXD peak of the (110) plane (□) for HDPE.

temperature, the difference between $t_{1/2H}$ and $t_{1/2T}$ became small. Furthermore, the X-ray diffraction peak from the crystal plane appeared after the crystallization exothermic peak under the experimental conditions. In the isothermal crystallization process of HDPE, the formation of trans-conformation occurred first and then the crystal growth process followed. Finally, perfection of the crystal packing occurred. Although the difference between $t_{1/2X}$ and $t_{1/2H}$ may come from the low sensitivity of the scintillation counter to scattering X-rays, it was proved that crystal lattice

formation took place after the formation of trans-conformation in the case of HDPE.

The conformation of HDPE in the molten state and the super-cooled liquid state was expected to be random. According to the degree of cooling from the equilibirium melting temperature, molecular conformation changed from the gauche-form to the trans-form to reduce the free energy of the system. Because this conformational transition probably occurred cooperatively in the molecule, the rate of conformational transition might be fast. When a long trans-conformation is formed in a molecule, molecular geometry changes from a random coil form to an extended form. With increasing fraction of the extended molecular part, the extended molecular parts align themselves by the excluded volume effect [24]. This process, which may be called the parallel ordering process [11] or the nematic transition [25], probably occurs in the initial stage of the nucleation process for HDPE.

4. Conclusion

The isothermal crystallization of $C_{36}H_{74}$ and HDPE from the molten state was observed by simultaneous DSC/FT-IR and DSC/WAXD measurements. The formation of trans-conformation and the crystal growth of the H-phase occurred at the same in the crystallization process of $C_{36}H_{74}$. The absorption band assigned to the rocking mode vibration of the methylene group was split at the transition from H-phase to C-phase. In the case of HDPE, the trans conformation was formed before the crystallization exothermic peak and X-ray diffraction peaks were observed. The conformational transition from gauche-form to trans-form was observed before the crystallization process of HDPE.

References

[1] L. Mandelkern, Crystallization of Polymers, McGraw-Hill, New York, 1964.
[2] H.N. Beck and H.D. Ledbetter, J. Appl. Polym. Sci., 9 (1965) 2131.
[3] T. Ozawa, Netsu Sokutei, 1 (1974) 2.
[4] K. Kamide and K. Fujii, Koubunshi Kagaku, 25 (1968) 155.
[5] J.R. Knox, in R.S. Porter and J.F. Johnson (Eds.), Analytical Calorimetry, Plenum Press, 1968, p. 45.
[6] H. Hatakeyama, H. Yoshida and J. Nakano, Carbohydr. Res., 47 (1976) 203.
[7] M. Takahashi, K. Umezaki, K. Fujiwara and H. Matsuda, *Netsu Sokutei*, 22 (1995) 16.
[8] M. Imai, K. Mori, T. Mizukami, K. Kaji and T. Kanaya, Polymer, 33 (1992) 4451.
[9] M. Imai, K. Mori, T. Mizukami, K. Kaji and T. Kanaya, Polymer, 33 (1992) 4457.
[10] M. Stamm, E.W. Fischer, M. Dettenmaier and P. Convert, Faraday Discuss. Chem. Soc., 68 (1979) 263.
[11] P.J. Flory, Proc. R. Soc. London, (1956) A234.
[12] G. Unger, J.L. Feijoo, A. Keller, R. Yourd and V. Percec, Macromolecules, 23 (1991) 3411.
[13] A.J. Ryan, J. Therm. Anal., 40 (1993) 887.
[14] H. Chung and M. Caffrey, Biophys. J., 63 (1992) 438.
[15] H. Yoshida and M. Takahashi, PF Activity Report, 10 (1992) 272.
[16] H. Takahashi and I. Hatta, Photon Factory News, 12 (1995) 21.
[17] H. Yoshida, PF Activity Report, 11 (1992) 272.
[18] H. Yoshida, R. Kinoshita and Y. Teramoto, Thermochim. Acta, 264 (1995) 173.
[19] H. Yoshida, Thermochim. Acta, (1995) 267 (1995) 239.

[20] T.K. Sallivan and J.J. Weeks, J. Res. Natl. Bur. Std., 74A (1970) 203.
[21] W. Piesczek, G.R. Strobl and K. Malzalm, Acta Crystallogr. Sect. B, 30 (1974) 1278.
[22] K. Takamizawa, Netsu Sokutei, 16 (1989) 112.
[23] S. Krimm, C.Y. Liang and G.B.B.M. Sutherland, J. Chem. Phys., 25 (1956) 549.
[24] P.J. Flory, Statistical Mechanics of Chain Molecules, John Wiley & Sons, New York, 1969, p. 35
[25] T. Shimada, M. Doi and K. Okano, J. Chem. Phys., 88 (1988) 2096.